

Supporting Information

Surface Sensitive Infrared Spectroelectrochemistry using Palladium Electrodeposited on ITO-Modified Internal Reflection Elements

Vi Thuy Thi Phan, Ian R. Andvaag, Nicole D. Boyle, Grace T. Flaman,
Bipinlal Unni, and Ian J. Burgess

¹ Department of Chemistry, University of Saskatchewan, Saskatoon, Saskatchewan, S7N 5C9 Canada

*corresponding author: email (ian.burgess@usask.ca)

Contents

Effective Medium Theory Calculations	2
<i>Modelling SEIRAS spectra</i>	2
<i>Effective Medium Theory (EMT)</i>	3
Palladium Delamination during Electrodeposition	5
Stability of Pd Covered ITO in Acidic and Basic Electrolytes	6
Linear Sweep Voltammetry during Potential Dependent ATR-SEIRA Measurement	7
Cyclic Voltammetry and Differential Capacity Measurements for the Pd Bead Electrode	8
Comparison of ATR-SEIRA Spectra using Au@ITO and Au on Si Films	9
Models of Pyridine and Pyridine Derivate Adsorption	10
References	11

Effective Medium Theory Calculations

Modelling SEIRAS spectra

The Fresnel equations¹ describe how light is reflected and transmitted at an interface between two different materials. Ohta *et al*² developed a transfer matrix formalism to propagate the Fresnel equations through a system of stratified layers. This enables the rapid calculation of the overall reflectivity and transmissivity of any system which is well-described as a stack of planar media, such as the thin films used in ATR-SEIRAS. A 4-layer system was constructed to match the experimental SEIRAS setup, and the parameters of this system are reported in Table S1.

Table S1 : System of stratified media to which the Fresnel equations can be applied to calculate the SEIRAS spectra.

Layer #	Material	Thickness (nm)	Source for calculating ϵ
1	Si	semi-infinite	Fixed $n=3.4$; $\kappa=0$
2	ITO	25	Drude model; $\nu_p=17000\text{ cm}^{-1}$; $\gamma=900\text{ cm}^{-1}$; $\epsilon_\infty=3.8$
3	Enhancing textured Pd	25	Bruggeman model, see details in Effective Medium Theory section
4	H ₂ O	semi-infinite	Tabulated n and κ values H ₂ O ³

The reflectivity for both s- and p-polarized light was calculated twice: once in the presence of the analyte (R_{samp}) and once in its absence (R_{ref}). A calculation analogous to experimental absorbance, which we call apparent absorbance, is calculated as $A_{app} = -\log(R_{samp}/R_{ref})$. This calculation is repeated as a function of IR frequency to obtain an absorbance spectrum and these spectra were calculated at different fill factors of Pd to generate the 2D plots presented in Figure 2 of the main text. The response for unpolarized light can be calculated by averaging the s- and p-polarized components.

The thickness of the Pd layer was estimated by first determining the maximum thickness of a

uniform palladium layer formed from the maximum electrodeposited charge, $Q_{\max} = 0.1 \text{ C cm}^{-2}$ using the atomic weight (106.42 g/mol) and density of Pd (12.02 g cm⁻³). This equates to an approximately 50 nm thick layer. As the EMT calculations were applied to different amounts of electrodeposited Pd, the average thickness (25 nm) was chosen for the layer thickness and the volume fraction of Pd was adjusted to account for the extent of deposited metal.

Effective Medium Theory (EMT)

The electrodeposited Pd used as the SEIRAS enhancing layer is not a uniformly smooth sheet of material, as is evidenced by the particles shown in the SEM images. The Fresnel equations are only valid for homogeneous media, but the SEIRAS film is an inhomogeneous composite of Pd nanoparticles, analyte molecules, and the electrolyte matrix. Since the nanoparticles of the film are significantly smaller than the wavelength of light used in a SEIRAS measurement, the composite Pd layer can be modelled as a homogenized material and the permittivity of this effective medium can be calculated using an EMT. We use the Bruggeman model for spherical particles to perform the homogenization:

$$\sum_{i=0}^n f_i \alpha_i = 0 \quad \#SI - 1$$

; where f_i is the fractional volume occupied by the i^{th} particle, and α_i is the polarizability for that particle. For spheres, the polarizability is given by:

$$\alpha_i = \frac{\epsilon_i - \epsilon_{BR}}{\epsilon_{BR} + \frac{1}{3}(\epsilon_i - \epsilon_{BR})} \quad \#SI - 2$$

; where ϵ_i is the permittivity of the i^{th} particle and ϵ_{BR} is the permittivity of the effective medium. Equation SI-2 is substituted into equation SI-1 and the resulting equation is solved for ϵ_{BR} . Each component material is treated as a separate type of spherical particle, and three components are necessary to describe the composite layer: metal, matrix, and analyte. The properties of these particles are summarized in Table S2. The properties provided in this table are used to calculate the effective permittivity of the homogenized medium.

Table S2 : The properties of the three components which constitute the composite enhancing metal layer.

Component	Material	Fill factor	Source for calculating ϵ_i
Metal	Pd	f_{Pd} (independent variable)	Tabulated n and κ values for Pd ⁴
Analyte	organic analyte	$f_a = 0.26 f_{Pd}$	Lorentz oscillator with parameters: $\nu_0=2175 \text{ cm}^{-1}$; $\nu_p=173 \text{ cm}^{-1}$; $\gamma=20 \text{ cm}^{-1}$; $\epsilon_\infty=1.77$
Matrix	H ₂ O	$f_{H_2O} = 1 - f_a - f_{Pd}$	Tabulated n and κ values H ₂ O ³

The fill fraction of Pd is fixed at a selected value. The analyte is assumed to be adsorbed to the surface of the Pd particles and therefore the fill fraction of the analyte should scale appropriately with the fill fraction of Pd. Even though the chosen Bruggeman model uses the polarizabilities of isolated spheres rather than core-shell structures, a core-shell model can be used to calculate the relative fill fraction of the analyte. The Pd enhancing film is treated as a monolayer of spheres having a diameter of 25 nm. The volume of the analyte is calculated as a 1 nm shell surrounding the 25 nm diameter Pd spheres. The fill fraction of the analyte can thus be computed as a function of the fill fraction of Pd. In the case of a 25 nm diameter Pd particle and a 1 nm shell, the fill fraction of the analyte is 26% of the fill fraction of Pd. The remaining volume not occupied by the Pd or the analyte is occupied by H₂O.

Palladium Delamination during Electrodeposition

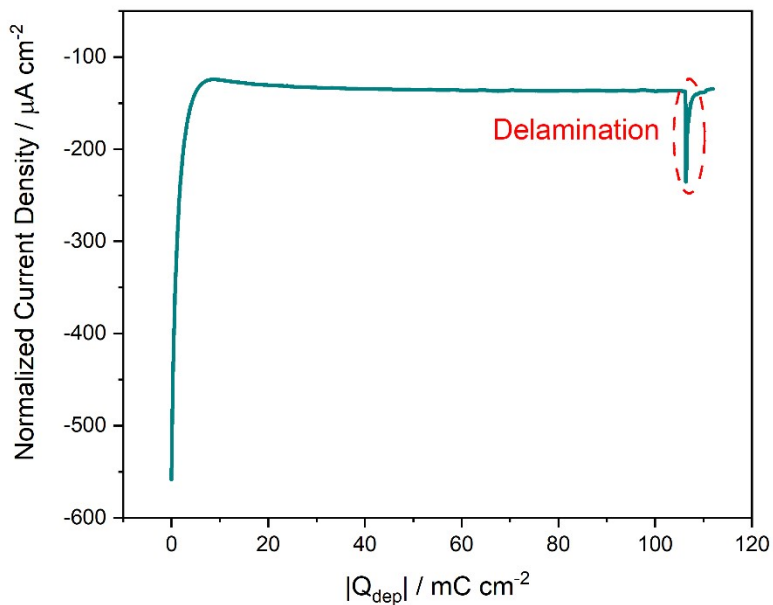


Figure S1 : The current density response as a function of the deposited charge (normalized by the geometric area of the exposed ITO surface) during constant potential electrodeposition of Pd from a solution of 0.1 M KCl and 1 mM K_2PdCl_4 on a Si face angled crystal modified by a 25 nm thick layer of indium tin oxide.

Stability of Pd Covered ITO in Acidic and Basic Electrolytes.

Cyclic voltammetry measurements were carried out in 0.1 M HClO₄ and 0.1 M KOH to test the stability of Pd/ITO films in strongly acidic and basic solutions. As seen in **Figure S2a**, the thickness of the double layer region from 0.1 V to 0.5 V is narrowed significantly after 50 scans in 0.1 M perchloric acid. However, the features attributed to Pd electrochemistry (Pd oxide and subsequent reduction of the oxide plus hydrogen discharge/oxidation) are actually enhanced with moderate potential scanning. We attribute the former observation to the known slow dissolution of bare ITO in strong acids. The latter observation indicates that the electrodeposited Pd protects the ITO underneath the Pd crystallites. Potential cycling acts as an electrochemical annealing step that actually improves the Pd electrochemistry. This positive effect is limited as extended potential cycling (for about 2h), led to complete loss of uncovered ITO and the loss of electrical conductivity. On the other hand, as shown in **Figure S2b**, the cyclic voltammetry of the Pd/ITO system is very stable over 50 scans in 0.1 M KOH. At the end of the experiment, the Pd layer was observed to remain intact and strongly adhered to the ITO layer. The conductivity was also unchanged. These results demonstrate that the Pd-ITO system is very stable and robust in strongly basic solutions.

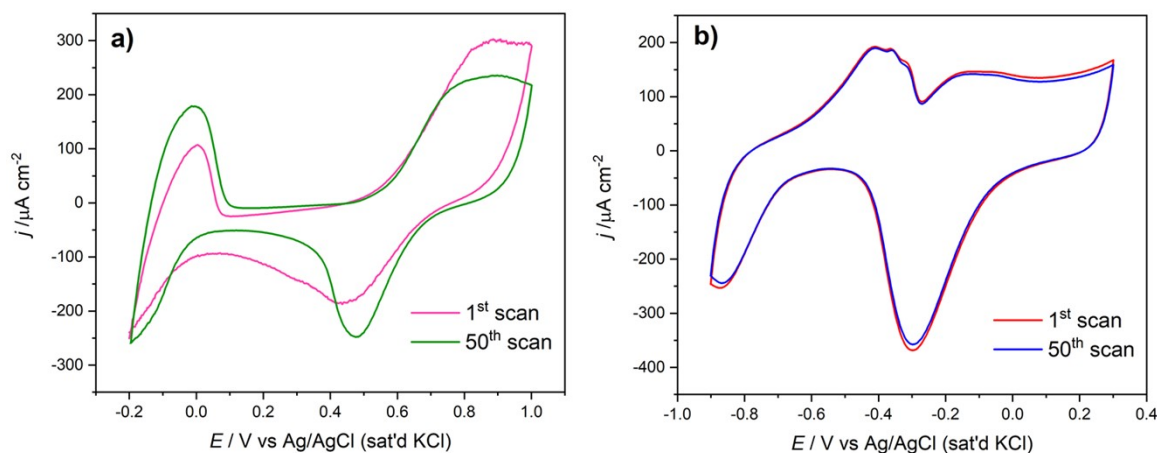


Figure S2 : Cyclic voltammograms of the Pd-modified ITO film (Pd deposition charge = 96 mC cm⁻²) on the first scan and the fiftieth scan at 50 mVs⁻¹ in **(a)** 0.1 M HClO₄ and **(b)** 0.1 M.KOH

Linear Sweep Voltammetry during Potential Dependent ATR-SEIRA Measurement

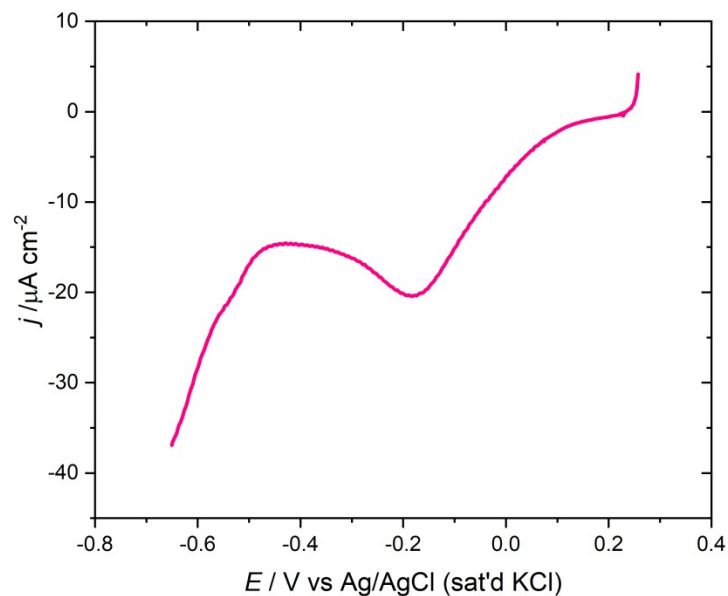


Figure S3 : Linear sweep voltammogram from OCP (0.26 V) to -0.65 V at 2 mV s^{-1} recorded during the potential dependent ATR-SEIRA measurement on a Pd-modified ITO film (Pd deposition charge = 96 mC cm^{-2}) in the mixture of 0.1 mM 4-methoxypyridine and 0.1 M KClO_4 .

Cyclic Voltammetry and Differential Capacity Measurements for the Pd Bead Electrode

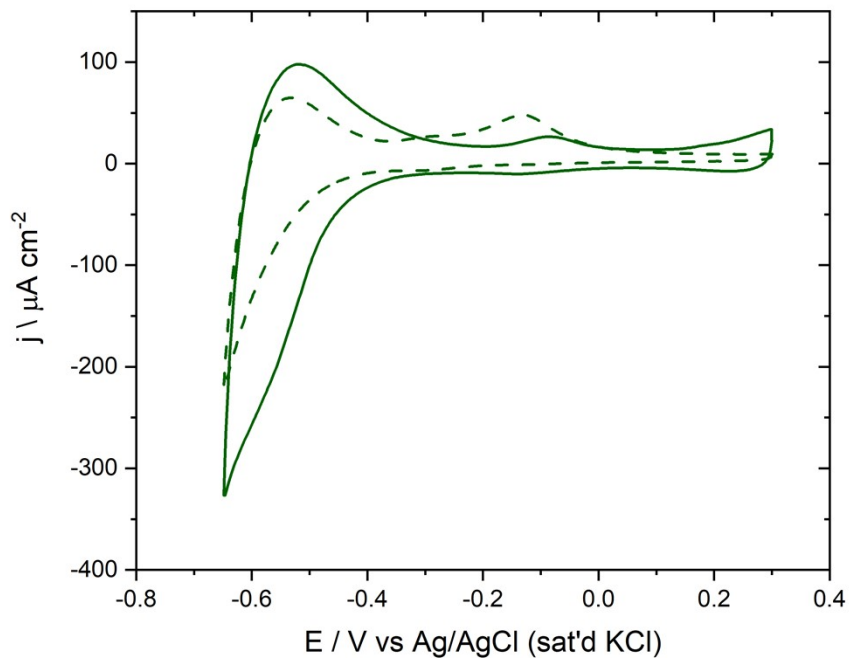


Figure S4 : Cyclic voltammograms in 0.1 M KClO_4 for the Pd bead electrode in the absence (solid line) and presence (dashed line) of 0.1 mM 4-methoxypyridine at 20 mV s^{-1} .

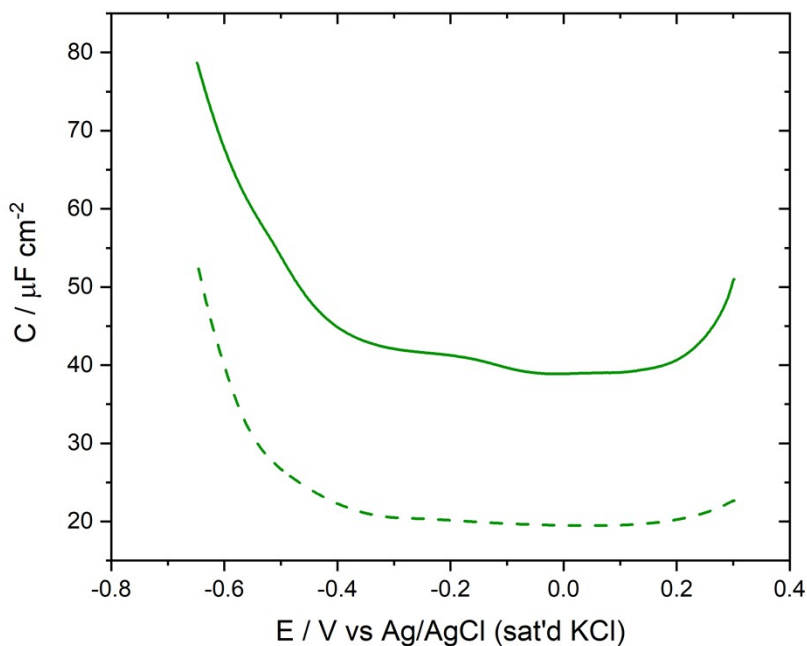


Figure S5 : Differential capacity curves in 0.1 M KClO_4 in the negative-going scan from 0.3 V to -0.65 V for the Pd bead electrode in the absence (solid line) and presence (dashed line) of 0.1 mM 4-methoxypyridine at 5 mV s^{-1} .

Comparison of ATR-SEIRA Spectra using Au@ITO and Au on Si Films

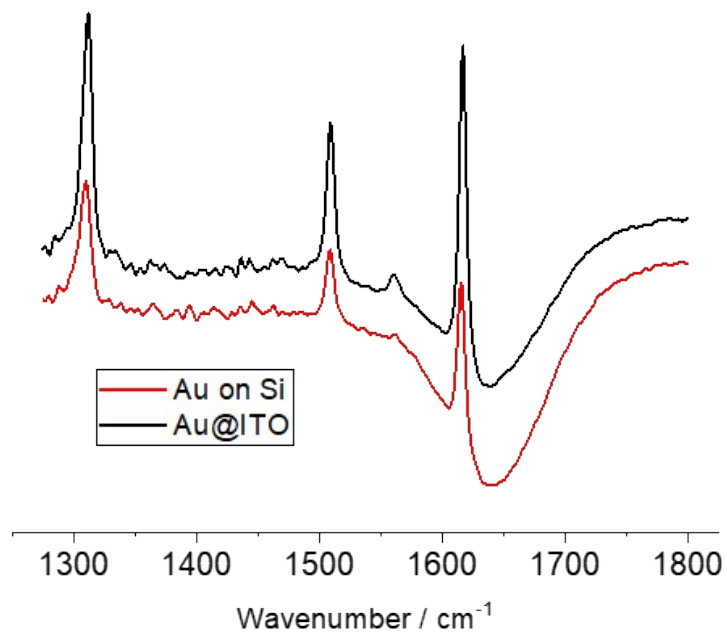


Figure S6 : ATR-SEIRA spectra for 0.1 mM 4-methoxypyridine in 0.1 M KClO₄ collected at 0.3 V vs. Ag/AgCl (sat'd KCl) on a gold film deposited directly on a Si IRE (red line) and Au-modified ITO island film (black line). Reference spectra were taken at - 0.9 V vs. Ag/AgCl (sat'd KCl) in the same solution.

Models of Pyridine and Pyridine Derivate Adsorption

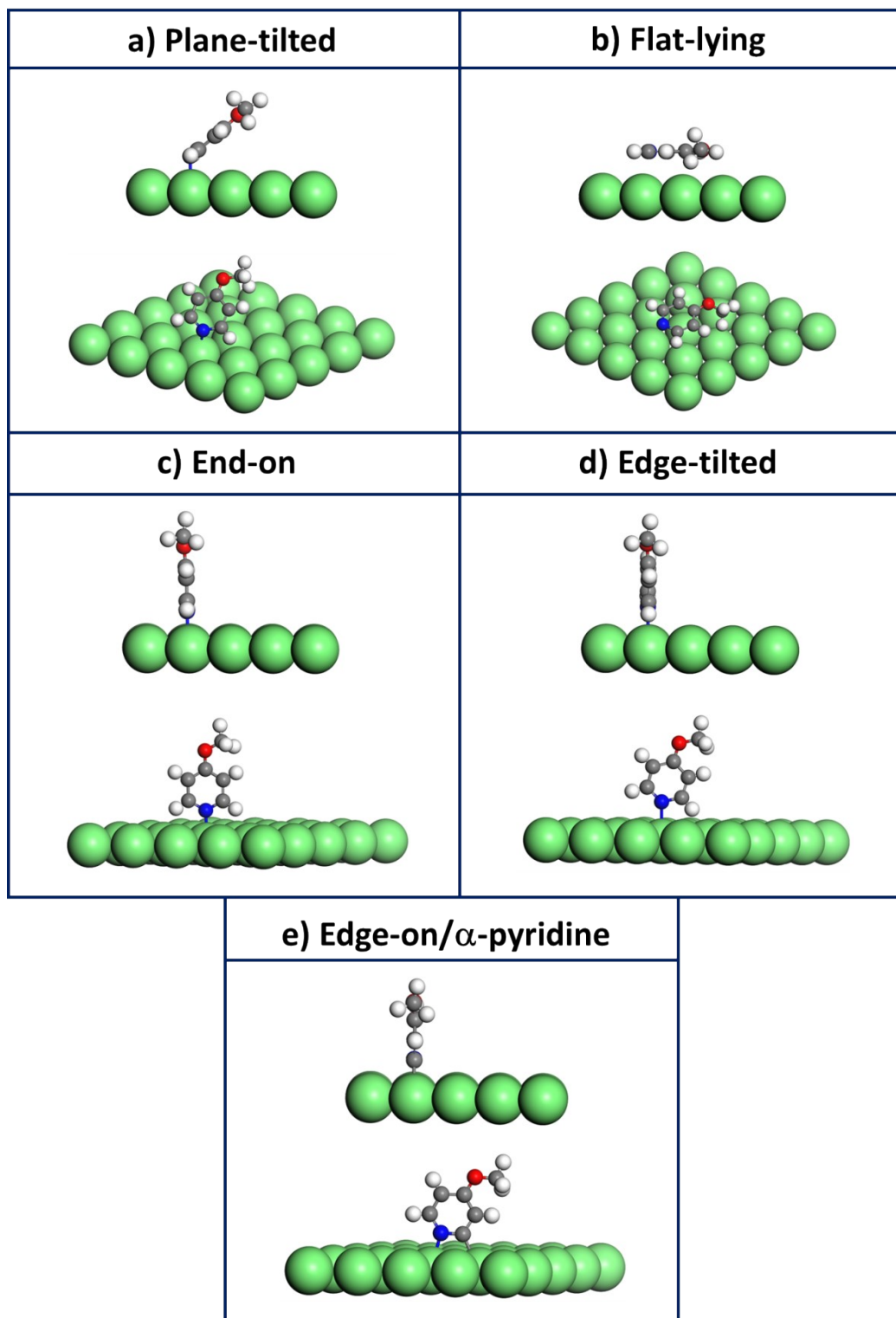


Figure S7 : Five adsorption configurations of 4-methoxypyridine (MOP) as the representative of the pyridine family on the metal surface, namely (a) plane-tilted, (b) flat-lying, (c) end-on, (d) edge-tilted and (e) edge-on/ α -pyridine species

References

1. de Sénarmont, H. H.; Verdet, E.; Fresnel, L. e. F., *Oeuvres Complètes D'Augustin Fresnel*. Imprimerie Impériale: 1866.
2. Ohta, K.; Ishida, H., Matrix formalism for calculation of electric field intensity of light in stratified multilayered films. *Applied optics* **1990**, 29, 1952-1959.
3. Hale, G.; Querry, M., Bladder cancers respond to EGFR inhibitors. *Cancer Discov* **2014**, 4, 980-981.
4. Borghesi, A.; Piaggi, A. Palladium (Pd). In *Handbook of Optical Constants of Solids*; Elsevier: 1997, pp 469-476.